Self-broadened half-widths and self-induced line shifts for water vapor transitions in the 3.2–17.76 μm spectral region via complex Robert–Bonamy theory

Bobby K. Antony, Robert R. Gamache *

Department of Environmental, Earth and Atmospheric Sciences, University of Massachusetts Lowell, 265 Riverside Street, Lowell, MA 01854-5045, USA
University of Massachusetts School of Marine Sciences, 265 Riverside Street, Lowell, MA 01854-5045, USA

Abstract

Water vapor in the Earth's atmosphere is being studied in the 3.2–17.76 μm spectral region by the atmospheric infrared sounder (AIRS) on Aqua, the troposphere emission spectrometer (TES) and the high-resolution dynamics limb sounder (HIRDLS) on Aura, both part of the NASA EOS mission. However, the lack of sufficient data on spectral parameters will hamper the prospect of accurate retrievals of temperature and concentration profiles. The spectral parameters for thousands of water vapor transitions are required, which are hard to determine by measurements alone. As reported previously [Can. J. Chem. 82 (2004) 1013–1027], of the 10 602 measurements of H_2O self-broadening half-widths only 440 intercomparisons with more than 3 data points have estimated uncertainty less than 10%. In this work, we have employed the mean relative thermal velocity approximation of the complex implementation of Robert–Bonamy formalism to obtain the self-broadened half-widths and self-induced line shifts for 5442 water vapor transitions in the 3.2–17.76 μm region. The calculations are compared with the measurement database and trends in the half-widths and line shifts are studied.
© 2006 Elsevier Inc. All rights reserved.

Keywords: Complex Robert–Bonamy formalism; Half-width; Line shift; Spectral lines; H_2O; Self broadening; Temperature dependence of half-width

1. Introduction

The number and range of predicted future scenarios due to global warming [1] has made us to think more closely on the Earth system. To understand such a complex system a clear picture on the cause-and-effect relationships between lands, oceans and atmosphere must be obtained. However, our knowledge is very limited about the impact of anthropogenic forcings and its effect on the climate change. To study these effects the entire globe must be surveyed over a long period of time. The data thus collected may be used to construct computer models to predict the cause-and-effect of climate change. One of the principal roles of NASA's Earth Observing System (EOS) is to collect data using its remote sensing satellites, to be used as input to climate models. The interpretation of remote sensing measurements, the retrieval of temperature and concentration profiles, and study of the radiative properties of the atmosphere from these remote sensed data are modeled using the absorption coefficients of atmospheric gases. The absorption coefficients, in turn, can be determined from knowledge of spectral parameters of the gases present. Water vapor is the strongest absorber of infrared radiation in the terrestrial atmosphere and is therefore one of the most important gasses controlling Earth's surface temperature. There are over 60 000 significant atmospheric spectral transitions for the isotopologues of H_2O ranging from microwave to the visible range of the spectrum. (More information on NASA's Aqua and Aura satellite missions can be found on the website http://eospso.gsfc.nasa.gov/eos_homepage/mission_profiles/index.php).

* Corresponding author. Fax: +1 978 934 3069.
E-mail address: Robert_Gamache@uml.edu (R.R. Gamache).

The spectroscopic parameters [2,3], i.e. the vacuum wavenumber of a molecular quantum transition, the corresponding transition intensity, the half-width and line shift of the transition, and the lower state energy, describe the absorption coefficient. These parameters and their temperature dependence are the basics to the understanding of our atmosphere. Proper knowledge of the spectral parameters helps to construct accurate computer models which enable us to forecast the cause and effect of climate changes. Of the parameters needed for inverting spectroscopic remotely sensed data, the collision-broadened half-width is the least well known [4]. The effects of uncertainty in half-width on the accuracy of retrieved parameters are well understood [5–7]. Also, the importance of the line shift is now understood [8,9], however the effects of the uncertainty on the retrieval are not as important as those of the half-width.

The half-width that one uses in simulating the spectrum is that for the mixture of gases present. Thus in the terrestrial atmosphere the half-width has components from nitrogen- and oxygen-broadening, given as the air-broadened value in the databases [2,3], and a component from self-broadening. While the self-broadening component is smaller than that of air-broadening it must be taken into account if one is trying to reach the uncertainty criteria established by the spectroscopic and remote sensing communities [4,10–12]. Currently, many radiative transfer codes use a table of self-broadened half-widths for water vapor that was generated by averaging a small number of measurements as a function of the rotational quantum number J.

The complex Robert–Bonamy (CRB) formalism [13,14] has been successful in predicting the half-width and line shift for self and foreign broadened spectral lines of many molecular systems. This method is used here to make calculations on the water vapor transitions in the spectral region from 3.2 to 17.76 μm (3124.2–563.2 cm^{-1}) at temperatures of 225 and 296 K. From the calculations the temperature dependence of the half-width can be determined. In a previous work Antony et al. [15] studied the effects to the self-broadened half-width by changes in rotational state, vibrational state, intermolecular potential, collision dynamics, and method of calculation. The calculations made here are based on that work and the results compared with measurements from the self-broadening of water vapor database [16].

2. Theory

2.1. General theory

The present calculations are based on the complex Robert–Bonamy formalism [13]. A detailed description of the theory and its derivations may be found in [14,17,18] and references therein. Here only the necessary equations and the salient features of the method are presented. In this approach the half-width and line shift for a ro-vibrational transition $f \leftarrow i$ are calculated by the formalism given by the real and imaginary part of the expression,

$$(\gamma - i\delta)_{f \leftarrow i}$$
$$= \frac{n_2}{2\pi c} \left\langle v \times \left[1 - e^{-{}^R S_2(f,i,J_2,v,b)} e^{-i[{}^I S_1(f,i,J_2,v,b) + {}^I S_2(f,i,J_2,v,b)]} \right] \right\rangle_{v,b,J_2}$$

$$(1)$$

where, n_2 is the number density of perturbers and $\langle \ldots \rangle_{v,b,J_2}$ is the average over all trajectories (with impact parameter b and initial relative velocity v) and initial rotational state J_2 of the collision partner. The real S_1 and complex $S_2 = {}^R S_2 + i{}^I S_2$ are the first and second order terms in the expression for the scattering matrix. S_1 and S_2 depend on the ro-vibrational states (and the associated collision induced transitions between these levels), the intermolecular potential and the collision dynamics involved. The complete expressions for these terms are explicitly defined in references [13,14,17,18].

The two features that have been incorporated in the present CRB formalism are; (i) the elimination of the cut-off procedure, and (ii) the better modeling of close collisions. The cut-off procedure adopted by earlier theories [19,20] was eliminated by the use of linked-cluster techniques [21]. The close intermolecular collisions (small b) are now very well defined by (a) the dynamics, which is second order in time producing curved trajectories based on the isotropic part of the intermolecular potential, and (b) the short range (Lennard–Jones) atom–atom potential, which is an important component for a proper description of pressure broadening, especially in the case of weekly interacting molecules [22].

The present calculation for the line shape parameters uses the mean relative thermal velocity ($\tilde{v}$) approximation (mrtv) to the CRB equations. It is estimated that mrtv approximation gives results 30–50 times faster than the velocity averaged results with a difference between the two methods of computation being only a few percent at ∼300 K for the system considered here [23].

2.2. The potential

The term S_1, a purely imaginary part of Eq. (1), is isotropic in the absence of any vibrational dependence of the anisotropic intermolecular forces. It has the label of the vibrational dephasing term and arises only for transitions where there is a change in the vibrational state. The potential leading to S_1 is given in terms of the isotropic induction and London dispersion interactions given as,

$$V_{\text{iso}}^{\text{induction}} = -\frac{\mu_1^2 \alpha_2}{R^6} \tag{2}$$

and

$$V_{\text{iso}}^{\text{dispersion}} = -\frac{3}{2} \frac{I_1 I_2}{I_1 + I_2} \frac{\alpha_1 \alpha_2}{R^6} \tag{3}$$

where μ_1 is the dipole moment of the radiating molecule and α_k and I_k are the polarizability and ionization potential of the radiator ($k = 1$) and perturber ($k = 2$). For water vapor the vibrational dependence of Eqs. 2 and 3 is contained in μ_1 (by Shostak and Muenter [24] in Debyes) and α_k (by Luo et al. [25] in au) given respectively as,

$$\mu = 1.855 + 0.0051\left(v_1 + \frac{1}{2}\right) - 0.0317\left(v_2 + \frac{1}{2}\right)$$
$$+ 0.0225\left(v_3 + \frac{1}{2}\right) \tag{4}$$

and

$$\alpha = 9.89 + 0.29\left(v_1 + \frac{1}{2}\right) - 0.03\left(v_2 + \frac{1}{2}\right)$$
$$+ 0.28\left(v_3 + \frac{1}{2}\right) \tag{5}$$

with v_n the number of quanta in the nth normal mode.

The complex valued $S_2 = {}^R S_2 + i^I S_2$ results from the anisotropic interaction potential with leading electrostatic components and atom–atom terms. The atom–atom potential is defined as the sum of pair wise Lennard–Jones (6–12) [26] interactions between atoms of the radiating and perturbing molecules given by,

$$V^{\text{at–at}} = \sum_{i=1}^{n} \sum_{j=1}^{m} 4\varepsilon_{ij}\left\{\frac{\sigma_{ij}^{12}}{r_{1i2j}^{12}} - \frac{\sigma_{ij}^{6}}{r_{1i2j}^{6}}\right\} \tag{6}$$

where n and m are the number of atoms in molecules 1 and 2 and the subscripts $1i$ and $2j$ stands for the ith atom of molecule 1 and jth atom of molecule 2, respectively. The ε_{ij} and σ_{ij} are the Lennard–Jones parameters for the atomic pairs. The heteronuclear atom–atom parameters are constructed from the homonuclear atom–atom parameters (ε_i and σ_j) by the combination rules of Hirschfelder et al. [27] or Good and Hope [28]. The atom–atom distance r_{ij} is expressed as an expansion of the inverse of the centre of mass separation, R given by Sack [29]. As this expansion is truncated, sufficient order must be taken to ensure the convergence of calculated half-widths and line shifts [30]. In the present case we have tested the results up to 8th order for convergence. The values for the homonuclear atom–atom parameters (ε_i and σ_j) are tabulated in the Table 1.

2.3. The wavefunctions

The reduced matrix elements are evaluated using the wavefunctions determined by diagonalizing the Watson Hamiltonian [31] in a symmetric top basis for the vibrational states involved in the transition for the radiator H_2O. The Watson constants are obtained from Matsushima et al. [32] for the ground state, from Camy-Peyret and Flaud [33] for the v_1, v_2, v_3, and $2v_2$ states and from Camy-Peyret and Flaud [34] for the $3v_2$ state.

Most of the molecular parameters used here for the water vapor system are well known and we have used the best available values from the literature. The multipole moments, rotational constants, polarizability and ionization potential (IP) employed here are tabulated in Table 1, along with their references.

3. Calculations

Calculations were performed using the CRB formalism for each vibrational band for the systems at 296 and 225 K to get the half-widths and line shifts using Eq. (1). For self-broadening of water vapor, out of 13 622 transitions available in the 2001 HITRAN database [37], calculations have been performed for 5442 rotational transitions in 11 vibrational bands (with $J \leqslant 18$) in the spectral range 3.2–17.76 μm (3124.2–563.2 cm^{-1}). In the calculations the atom–atom potential is expanded to 8th order to insure convergence and the imaginary components are used. The number of lines considered in this work for each vibrational band of $H_2{}^{16}O$ in the wavenumber region is listed in Table 2.

4. Results and discussion

The calculations provide the half-width and line shift for self-broadening of the water vapor transitions with $J \leqslant 18$ in the 3.2–17.76 μm spectral range. There are a number of measurements of the self-broadened half-width [38–52] and self-induced line shift [52] for water vapor transitions in this spectral range. Below the calculations are compared with the measurement database.

Table 1
Electrostatic moments of H_2O and heteronuclear atom–atom Lennard–Jones (6–12) parameters for the collision pairs

Moments			
μ/esu [24]	Q_{xx}/esu [35]	Q_{yy}/esu [35]	Q_{zz}/esu [35]
1.8549×10^{-18}	-0.13×10^{-26}	-2.50×10^{-26}	2.63×10^{-26}
Ionization potential	12.6 eV [36]		
Atom–atom parameters			
Atomic pair	H–H	H–O	O–O
σ (Å)	2.683	2.565	3.010
ε/k_B (K)	11.25	24.13	51.73

Table 2
Rotational transition for each vibrational band for H_2O–H_2O

$v_1' v_2' v_3'$	$v_1'' v_2'' v_3''$	# lines
000	000	506
010	010	144
010	000	1885
020	010	872
100	010	532
030	020	382
001	010	484
020	000	326
030	010	146
100	000	90
001	000	75

4.1. Comparison with measurement

There are a number of transitions in the spectral range of this study for which multiple measurements have been made by different experimental groups. In such cases the average value of the measurements is determined and compared with the measurements as well as with the calculated value. For self-broadening of water vapor there are 221 transitions with pairs of measurements, 20 transitions with 3 measurements and 2 transitions with 4 measurements. In the comparison the average percent difference (APD) (experiment-calculation), the average absolute percent difference (AAPD), and the standard deviation (SD) are calculated. For the intercomparison of measurements, each measurement is compared with the average value of the measurements, hence the average percent difference is zero. The data are also compared as a function of vibrational band.

Table 3 presents the intercomparison of the measured data and the comparison of the average value of the measurements (when 2 or more data exist for the same transition) with the value from the CRB calculations. The first row gives the comparison of roughly one thousand data for which only a single measurement was available per transition. The APD is −4.31 with the AAPD of 5.85 indicating the calculations are giving results roughly 4% larger than the measurements. The standard deviation for these data is 6.23. Next we have pairs of points. For 221 transitions 2 measurements were made. The APD of the comparison of the average of the measurements to the calculations is −0.08. It is interesting to note that the AAPD and SD of the comparison of calculations with measurement are smaller than the intercomparison of the measurements. For 3 and 4 points there are fewer intercomparisons, 20 and 2 transitions, respectively. The 3 point data average compared with calculation gives an APD of 5.00, that for the 4 point data average has the APD equal to 9.91. For both these data sets, the SD and AAPD of the comparison of calculations with the average experimental values gives better agreement than the intercomparisons of the measurements.

In the region of this study, measurements have been made for five vibrational bands; rotation, v_2, v_2–v_2, $2v_2$–v_2, and v_1–v_2. Table 4 shows the results of the comparison with measurement. There are 1207 transitions in the 5 vibrational bands with an average absolute percent

Table 4
Vibrational band, number of measured and calculated lines, average percent difference (measurement-calculation), standard deviation, and average absolute percent difference

Band	# of lines		APD(exp − calc)	SD	AAPD
	Exp	CRB			
000–000	121	117	0.27	10.09	6.06
010–000	1115	853	−3.12	6.72	5.72
010–010	2	2	−0.85	14.57	10.30
020–010	205	204	−6.21	3.95	6.50
100–010	31	31	−4.80	3.32	4.85

difference of roughly 5 to 6. The AAPD does not vary much from band to band with the exception of the v_2–v_2 band for which there are only 2 transitions compared.

The comparison with the self-broadening measurement database gives confidence in the CRB calculation results. And while the AAPDs are roughly the same from band to band the APD values reported in Table 4 indicate that a simple scaling of the calculations is inappropriate.

Toth et al. [52] have made line shift measurements for 1136 transitions belonging to 5 vibrational bands in the spectral region 590–2400 cm^{-1}. Most of the data are for the rotation and v_2 bands with additional data for the $2v_2$–v_2, v_1–v_2, and v_2–v_2 bands. These data are compared with the calculations. Due to the small magnitude of the line shifts (the uncertainty can be larger than the measured shift) the comparison uses the difference between the measurement and the calculated value. The difference has been plotted in Fig. 1 versus the absolute value of the measured line shift in cm^{-1} atm^{-1}. The differences are clustered about zero with values as large as 0.05 cm^{-1} atm^{-1}. Table 5 shows the statistics of the comparison as a function of vibrational band and overall. The agreement between measurement and calculations is good. The table shows the poorest agreement is with the rotation band. This is the only band where the calculation does not have a purely vibrational contribution (the S_1 term). The line shift comes from the real and imaginary parts of the S_2 term. As discussed in previous works [53,54] the atom–atom parameters have an uncertainty that results from the method used to determine them. It is expected that in the future better agreement will be obtained between measurement and calculations made using a better intermolecular potential.

Table 3
Average percent difference, standard deviation and average absolute percent difference for measurement versus average measurement and calculation versus average measurement for transitions measured by a single, two, three, and four groups

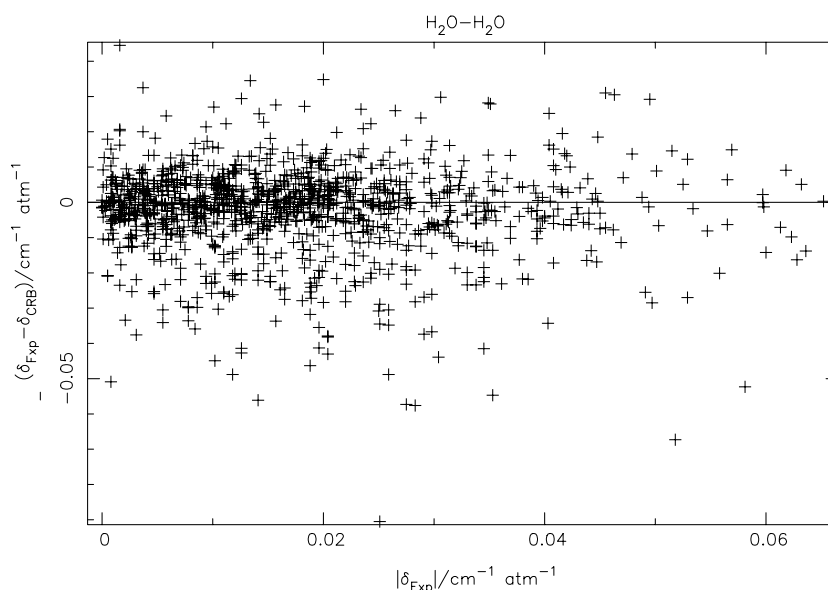| # measured data per transition	# data measured	# data calculated	Ave % diff (exp − calc)	SD		|Ave PD|	
				Exp	Calc	Exp	Calc
1	964	964	−4.31	0.00	6.23	0.00	5.85
2	442	221	−0.08	9.09	8.10	7.08	5.94
3	60	20	5.00	10.79	5.72	8.47	5.72
4	8	2	9.91	14.90	1.79	13.49	9.91

Fig. 1. The difference between the measured and calculated line shift, $(\delta_{exp} - \delta_{CRB})$, versus the absolute value of the measured line shift in $cm^{-1}\ atm^{-1}$.

Table 5
Comparison of measured and CRB calculated line shifts for the 5 vibrational bands studied by Toth et al. [52] Differences are measurement − calculation in units of $cm^{-1}\ atm^{-1}$

Band	# lines	Ave difference	Ave |difference|	SD
000–000	105	−0.0177	0.0200	0.0178
010–000	796	−0.0012	0.0071	0.0105
010–010	2	−0.0085	0.0085	0.0044
020–010	203	−0.0007	0.0090	0.0121
100–010	30	0.0059	0.0124	0.0149
Overall	1136	−0.0025	0.0088	0.0128

4.2. Dependence of the half-width and line shift on rotational states

In their work on self-broadening of water vapor transitions Toth et al. [52] looked at trends in the half-width and line shift as a function of the rotational quantum numbers. They listed their measurements according to "families" of transitions defined by ΔJ, ΔK_a, and K_a. Within a "family" of transitions the rotational quantum numbers obey the following rules" ΔK_a and K_a'' are the same and ζ'' is 0 or 1 where

$$\zeta = K_a + K_c - J \tag{7}$$

and the prime and double prime are the standard spectroscopic notation, upper and lower state, respectively. For example, the rotational transitions $1_{10} \leftarrow 0_{00}$, $2_{12} \leftarrow 1_{01}$, $3_{13} \leftarrow 2_{02}$, etc. correspond to a family. Toth et al. suggest that in most cases the half-widths follow a pattern within a "family" from which they determine "smoothened values" that can be used when data are not available.

Here we investigate how recognizable the pattern is within a "family" and ask to what extent are the smoothened values useful given the needs of the spectroscopic and remote sensing communities [4,10–12]. This is done using the calculations for the v_2 band for which 1885 transitions were considered. Plots were made for the "families" where the half-width in $cm^{-1}\ atm^{-1}$ is plotted versus J''. Plots were made for $K_a'' = 0$–13, $|\Delta K_a| = 1$ and 3, for P-, Q-, and R-transitions, and $\zeta = 0$ or 1. Typical examples are shown in Figs. 2 and 3 where the half-width is plotted versus J'' for transitions with $\Delta K_a = \pm 1$, $K_a'' = 3$ and $\zeta = 0$ for R-type (Fig. 2) and Q-type (Fig. 3) transitions. In the figures the symbols are the sign of ΔK_a. While some trend is evident, it is apparent that "smoothened values" extracted from such a plot will have high uncertainty. In addition the structure appears and disappears for different values of K_a''. It should also be pointed out that the points used to determine smoothened values have associated error thus increasing the uncertainty in the "smoothened values".

Toth et al. stated that at first inspection the pressure shifts appeared to have no smooth behavior as a function of the quantum numbers. However, closer inspection of subset pairs of *families* revealed structure in the shifts and for the vibrational bands they considered transition pairs with the rotational quantum numbers and the reversed set of rotational quantum numbers often have shifts that are opposite in sign.

Their finding is not a surprise. Theoretically it is known that the line shift is comprised of several components in terms that compete with each other [53]. The line shift is strongly dependent on the vibrational transition in question through the S_1 term. The imaginary part of the S_2 term also contributes and within the same band the parts for the upper and lower state change sign when rotational reversal is done. In addition the real part of the S_2 term damps out the $\sin[S_1 + \text{Im}(S_2)]$ term as $\text{Re}[S_2]$ gets large. These findings suggest that from transition to transition in a *family* the line shift may not follow a smooth line. To see if this
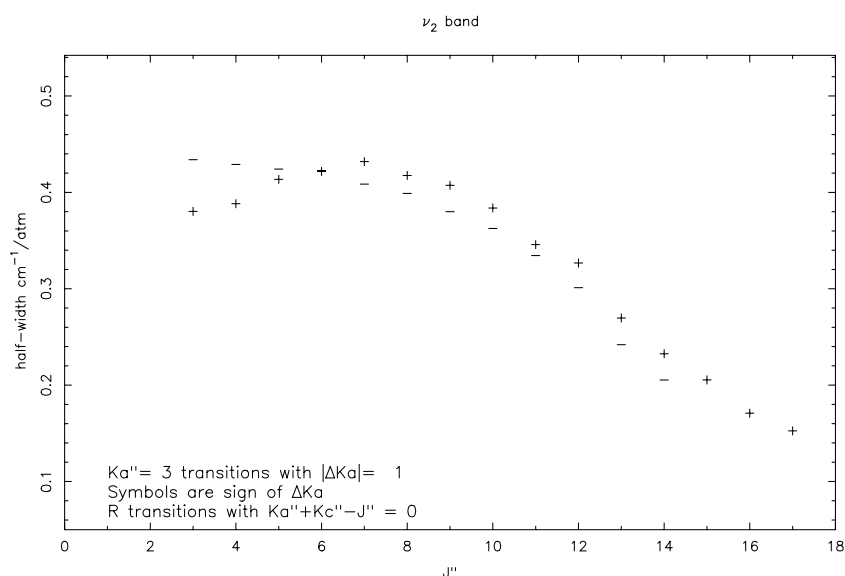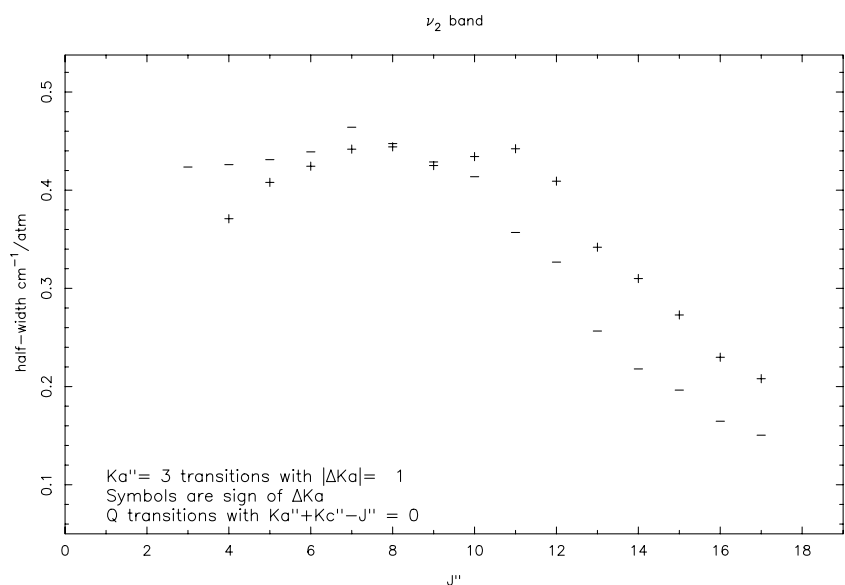
Fig. 2. The half-width for the *family* of transitions with $\Delta K_a = \pm 1$, $K''_a = 3$, $\zeta = 0$, and R-type transitions in the ν_2 band versus J''. In the figures the symbols are the sign of ΔK_a.

Fig. 3. The half-width for the *family* of transitions with $\Delta K_a = \pm 1$, $K''_a = 3$, $\zeta = 0$, and Q-type transitions in the ν_2 band versus J''. In the figures the symbols are the sign of ΔK_a.

conjecture is true plots were again made for the *families* as discussed above where now the line shift is plotted versus J''. Fig. 4 is an example for Q-type transitions with $\Delta K_a = \pm 1$, $K''_a = 3$ and $\zeta = 0$. In the figures the symbols are the sign of ΔK_a. For both the $\Delta K_a = 1$ and -1 the curves are not smooth with the line shift jumping up and down and often changing sign. One can see here, and in other plots that were made, that if only a subset of the data are plotted it can give an appearance of smooth behavior.

In another measure to increase the database of half-widths, Toth et al. [52] used the fact that the half-widths for transitions where the rotational quantum numbers are

reversed, i.e. $J'_{K'_a K'_c} \leftarrow J''_{K''_a K''_c}$ and $J''_{K''_a K''_c} \leftarrow J'_{K'_a K'_c}$, are often observed to be similar to each other. Note, in their study Toth et al. assumed the vibrational dependence of the half-width was negligible. It is now understood that in certain classes of transitions the vibrational dependence of the half-width can be strong [53]. However, the off-resonance effects that lead to the strong vibrational dependence are not realized in self-broadening of water vapor since there are always some on resonance collisions leading to the half-width [15]. Toth et al. found that the differences between the half-width of a transition and that from the rotational reversed state are often less than 10% even when considering the ground and hot bands.
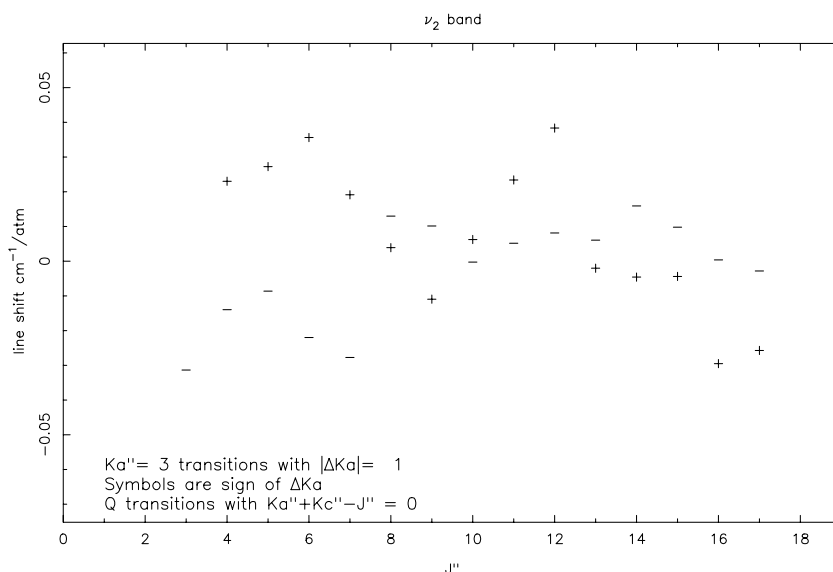
Fig. 4. The line shift for the *family* of transitions with $\Delta K_a = \pm 1$, $K''_a = 3$, $\zeta = 0$, and Q-type transitions in the ν_2 band versus J''. In the figures the symbols are the sign of ΔK_a.

Here the use of rotational reversal to estimate the half-width was investigated again using the data for the ν_2 band. The data were taken and the half-widths for transitions $J'_{K'_a K'_c} \leftarrow J''_{K''_a K''_c}$ with data for the corresponding reversed transition $J''_{K''_a K''_c} \leftarrow J'_{K'_a K'_c}$ was considered. This yielded 827 pairs of transition-reversed transition. The percent difference between the two half-widths was determined and plotted versus the magnitude of the half-width. These data are plotted in Fig. 5. While the percent difference for a good number of transitions fall between ±10% (660 points) as reported by Toth et al. many go to ±20% (167 points). The average absolute percent difference, 6.33, is larger than

the uncertainty desired by the spectroscopic and remote sensing community.

The study of Toth et al. suggested that the line shift of a rotationally reversed transition is minus that of the original transition. The data for the ν_2 band was taken and the ration of the line shift for a transition and the rotational reversed transition was formed. In Fig. 6 this ratio is plotted versus the magnitude of the line shift. If the conjecture of Toth et al. is correct one should expect to see a confluence of points along a line equal to −1. This is clearly evident in the figure, but there are many points that are not close to the line at −1. In fact the ordinate axis limits are
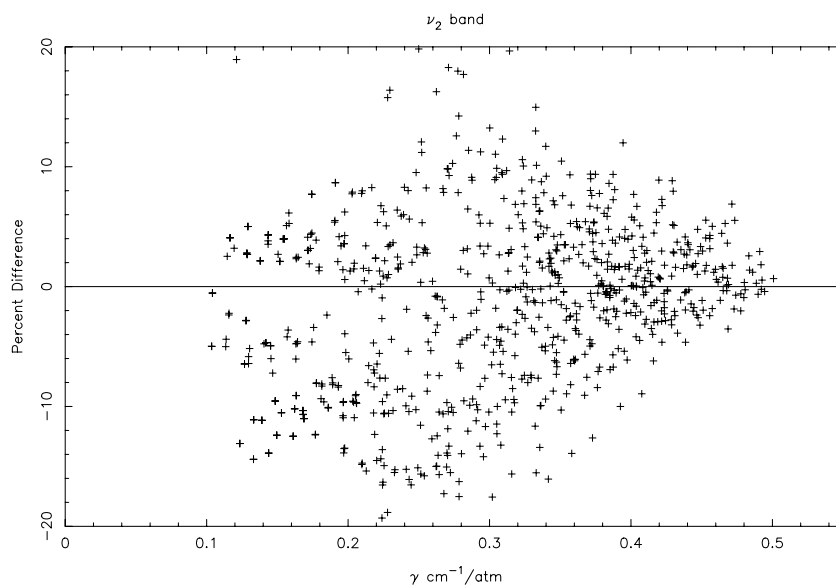

Fig. 5. The percent difference between the half-width for a transition in the ν_2 band and that from the transition with the rotational quantum numbers reversed versus the magnitude of the half-width in cm^{-1} atm^{-1}.
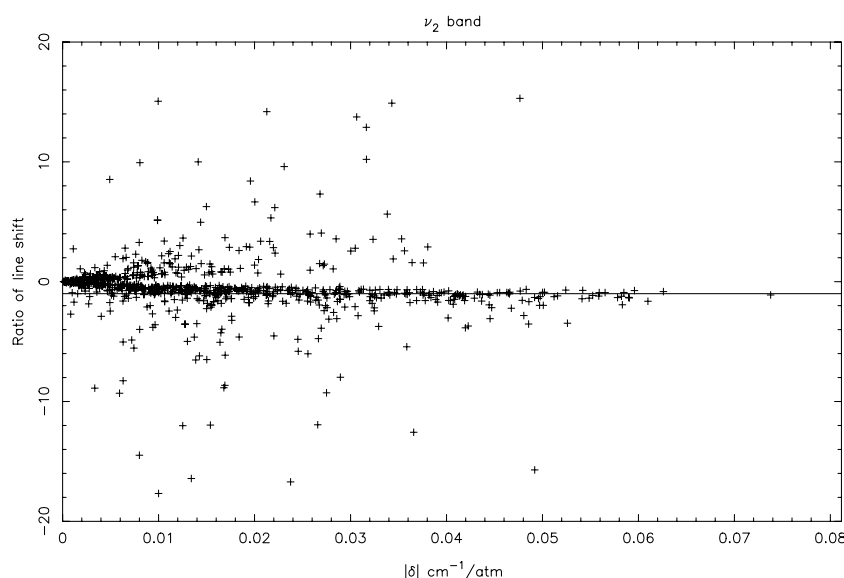
Fig. 6. The ratio of the line shift for a transition in the ν_2 band and that from the transition with the rotational quantum numbers reversed versus the magnitude of the line shift in cm^{-1} atm^{-1}.

set to ±20 in Fig. 6, where as in the original figure the range in the ratios is from -100 to $+200$. The average ratio for the 827 points is -1.33 indicating that the conjecture of Toth et al. is reasonable. However, given the number of transitions where the ratio is not close to -1 indicates that using this method to predict line shifts will lead to large error.

4.3. Temperature dependence of the half-width

The temperature dependence of the half-width is generally given in terms of the power law model,

$$\gamma(T) = \gamma(T_0)\left[\frac{T_0}{T}\right]^n. \tag{8}$$

However, for certain types of radiator-perturber interactions the power law model is being questioned. Wagner et al. [55] have shown that for certain transitions of water vapor perturbed by air, N_2 or O_2 the power law does not correctly model the temperature dependence of the half-width. This fact was also demonstrated by Toth et al. [56] in a study of air-broadening of water vapor transitions in the region from 696 to 2163 cm^{-1}. In both studies it was found that the temperature exponent, n, can be negative for many transitions. In such cases the power law, Eq. (8), is not valid. The mechanism leading to negative temperature exponents was discussed by Wagner et al. [55], by Antony et al. [15], and by Hartmann et al. [50] and is called the resonance overtaking effect. Antony et al. showed that for self-broadening of water vapor that there are always enough collisions that are on resonance where the resonance overtaking effect can be neglected. Thus for the H_2O–H_2O system the power law is a reasonable fit to the data and the temperature dependence can roughly be determined by two temperatures.

Here, calculations were made for the 5442 transitions in the spectral region of the study at 225 and 296 K. From these values the temperature exponent was determined for each transition. It is estimated that the uncertainty of the temperature exponents derived from the two temperatures is not greater than 10–15%. Fig. 7 shows the temperature exponent for all transitions studied versus $J'' + 0.9(K_a''/J'')$. The factor added to J'' is to spread the points out according to the oblate-prolate limit of the states. Birnbaum [57] has shown that for a system that has only the "dipole–dipole" interaction, the temperature exponent is 1.0. H_2O–H_2O has been thought of as a "dipole–dipole" system. Indeed the study of Antony et al. [15] demonstrated that H_2O–H_2O behaves as a "dipole–dipole" interacting system in many ways. The temperature exponents in Fig. 7 range from ~0.95 to 0.1 showing a large variation from the value for a pure "dipole–dipole" system and from the average temperature exponent of 0.54.

The temperature exponent for like rotational quantum numbers and different vibrational quantum numbers were compared for 1194 rotational transitions involving 3867 points. For each rotational transition the percent difference from the average temperature exponent of the group was determined. The results show that there is a small vibrational dependence with differences generally of order $\pm5\%$ for different vibrational bands. The average absolute error for the comparison is 4% with some values as large as $\sim \pm 35\%$.

The temperature exponent data were studied to see if there was any structure with respect to the *families* of transitions and if the structure, if any, could be used to predict values not in the data. Plots were made for $K_a'' = 0$–13, $|\Delta K_a| = 1$ and 3, for P-, Q- and R-transitions, and $\zeta = 0$ or 1. Fig. 8 shows the temperature exponent versus J'' for transitions with $\Delta K_a = \pm1$, $K_a'' = 2$ and $\zeta = 0$. In the figure
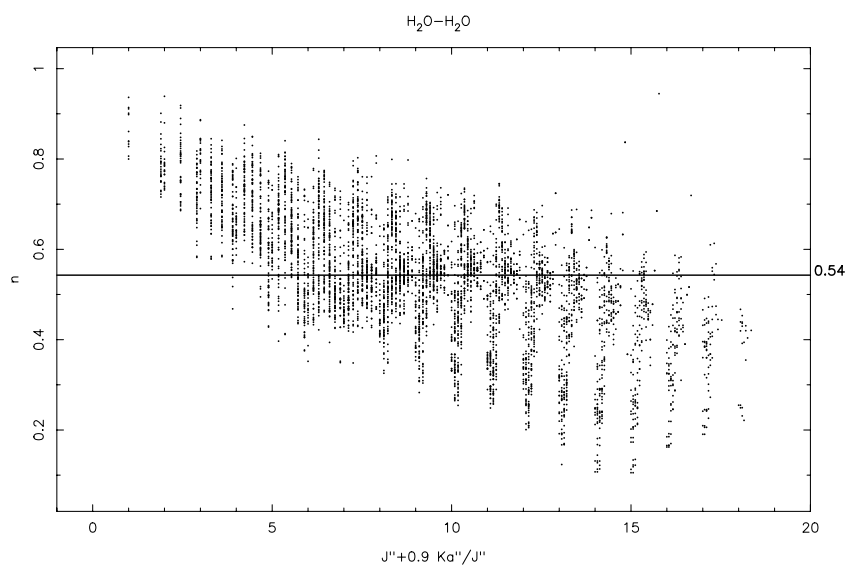
Fig. 7. The temperature exponent for all transitions studied versus $J'' + 0.9(K_a''/J'')$. The factor added to J'' is to spread the points out according to the oblate-prolate limit of the states.

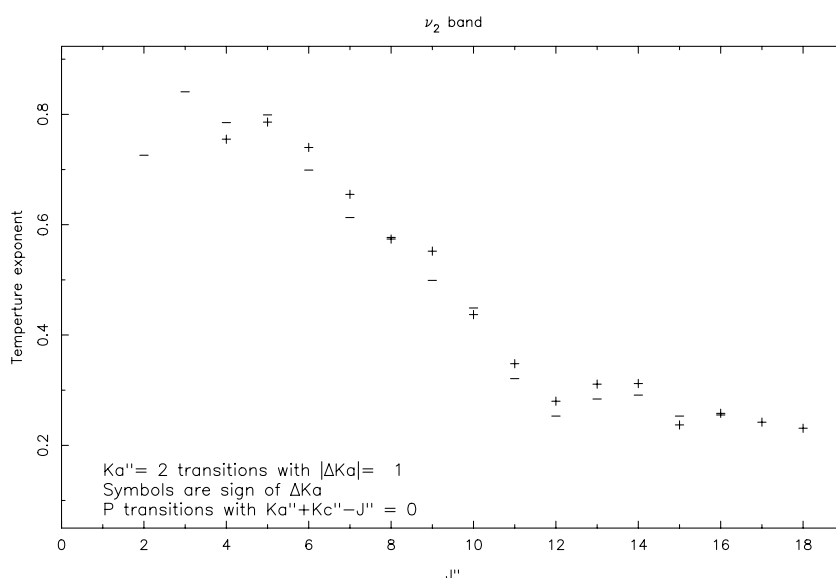
Fig. 8. The temperature exponents for the *family* of transitions with $\Delta K_a = \pm 1$, $K_a'' = 2$, $\zeta = 0$, and P-type transitions versus J''. In the figure the symbols are the sign of ΔK_a.

the symbols are the sign of ΔK_a. While some structure is evident, it is not smooth and cannot be used to predict missing data especially when parts of the data set are missing.

5. Summary and conclusion

Half-width and line shift calculations were made for transitions (with $J \leqslant 18$) of the principal isotopologue of water vapor in the region 3.2–17.76 μm at 225 and 296 K using the complex implementation of the Robert–Bonamy theory. These calculations give the line shape parameters for 5442 rotational transitions in 11 vibrational bands in the spectral range. The calculations were compared with the measurement database for self-broadening and

self-induced line shifts [16]. The calculated half-widths agree with the measurements as well as the measurements agree with each other. The line shifts agree well with the measurements of Toth [52] with the rotation band data showing the largest differences as discussed above.

The calculated data were divided into *families* of transitions and these *families* studied for trends in the half-width, line shift and temperature dependence of the half-width. There are some general trends. However, the structures change strongly for different K_a'' values making this method not very useful for predicting missing data. Reversal of the rotational quantum numbers was also studied to see if transitions related by rotational reversal have the same half-width and line shift. Here as well general trends could be seen but the number of transitions that do not obey the

trends is large. The result is that using rotational reversal to predict half-widths or line shifts does not yield valuable results.

The temperature dependence of the half-width was determined for the 5442 transitions of this study. The values range from ~0.95 to 0.1. The temperature exponents were studied with respect to the *families* of transitions. Again for some K_a'' values general trends can be seen but not for others. A small vibrational dependence of the temperature exponent was observed.

These data are available from one of the authors (http://faculty.uml.edu/Robert_Gamache/) or from the Supplemental data site of the Journal of Molecular Spectroscopy. The final self-broadened data file was given to Dr. Larry Rothman to be merged with the measured half-widths for addition to the HITRAN database.

Acknowledgments

Appendix A. Supplementary data

Supplementary data for this article are available on ScienceDirect (www.sciencedirect.com) and as part of the Ohio State University Molecular Spectroscopy Archives (http://msa.lib.ohio-state.edu/jmsa_hp.htm).

References

[1] IPCC Second Assessment – Climate Change 1995, A Report of the Intergovernmental Panel on Climate Change, B. Bolin, (Ed.), 1995, World Meteorological Organization, Geneva.

[2] L.S. Rothman, D. Jacquemart, A. Barbe, D.C. Benner, M. Birk, L.R. Brown, M.R. Carleer, C. Chackerian Jr., K. Chance, L.H. Coudert, V. Dana, V.M. Devi, J.-M. Flaud, R.R. Gamache, A. Goldman, J.-M. Hartmann, K.W. Jucks, A.G. Maki, J.-Y. Mandin, S.T. Massie, J. Orphal, A. Perrin, C.P. Rinsland, M.A.H. Smith, J. Tennyson, R.N. Tolchenov, R.A. Toth, J. Vander Auwera, P. Varanasi, G. Wagner, J. Quant. Spectrosc. Radiat. Transfer 96 (2005) 139–204.

[3] N. Jacquinet-Husson, E. Arie', J. Ballard, A. Barbe, G. Bjoraker, B. Bonnet, L.R. Brown, C. Camy-Peyret, J.-P. Champion, A. Che'din, A. Chursin, C. Clerbaux, G. Duxbury, J.-M. Flaud, N. Fourrie', A. Fayt, G. Graner, R.R. Gamache, A. Goldman, V. Golovko, G. Guelachvili, J.-M. Hartmann, J.C. Hilico, J. Hillman, G. Lefe'vre, E. Lellouch, S.N. Mikhailenko, O.V. Naumenko, V. Nemtchinov, D.A. Newnham, A. Nikitin, I. Orphal, A. Perrin, D.C. Reuter, C.P. Rinsland, L. Rosenmann, L.S. Rothman, N.A. Scott, J. Selby, L.N. Sinitsa, J.M. Sirota, M.A.H. Smith, K.M. Smith, V.G. Tyuterev, R.H. Tipping, S. Urban, P. Varanasi, M. Weber, J. Quant. Spectrosc. Radiat. Transfer 62 (1999) 205–254.

[4] A. Barbe, Proceedings of the Atmospheric Spectroscopy Applications Workshop, ASA REIMS 96, Université de Reims, Champagne Ardenne, 1996.

[5] M.A.H. Smith, L.L. Gordley, J. Quant. Spectrosc. Radiat. Transfer 29 (1983) 413–418.

[6] W.P. Chu, E.W. Chiou, J.C. Larsen, L.W. Thomason, D. Rind, J.J. Buglia, S. Oltmans, M.P. McCormick, L.M. McMaster, J. Geophys. Res. 98 (1993) 4857–4866.

[7] J.C. Liljegren, S.-A. Boukabara, K. Cady-Pereira, S.A. Clough, IEEE Trans. Geosci. Remote Sensing 43 (2005) 1102–1108.

[8] J. Margolis, Jet Propulsion Laboratory, private communication, 1997.

[9] H.C. Pumphrey, S. Buehler, J. Quant. Spectrosc. Radiat. Transfer 64 (2000) 421–437.

[10] C.A. Reber, NASA Goddard Space Flight Center Publication 430-1003-001, 1985.

[11] M.A.H. Smith, NASA Conference Publication 2396, NASA, Scientific and Technical Information Branch, 1985.

[12] M.A.H. Smith (ed.), Third Langley Spectroscopic Parameters Workshop, NASA Langley Research Center, Hampton, VA, 1992.

[13] D. Robert, J. Bonamy, J. de Phys. 20 (1979) 923–943.

[14] R.R. Gamache, R. Lynch, S.P. Neshyba, J. Quant. Spectrosc. Radiat. Transfer 59 (1998) 319–335.

[15] B.K. Antony, S. Neshyba, R.R. Gamache, J. Quant. Spectrosc. Radiat. Transfer, in press.

[16] R.R. Gamache, J.-M. Hartmann, Can. J. Chem. 82 (2004) 1013–1027.

[17] R. Lynch, R.R. Gamache, S.P. Neshyba, J. Quant. Spectrosc. Radiat. Transfer 59 (1998) 595.

[18] R. Lynch. Half-widths and line shifts of water vapor perturbed by both nitrogen and oxygen, Ph.D. dissertation, Physics Department, University of Massachusetts Lowell, June, 1995.

[19] P.W. Anderson, Phys. Rev. 76 (1949) 647–661.

[20] C.J. Tsao, B. Curnutte, J. Quant. Spectrosc. Radiat. Transfer 2 (1962) 41–91.

[21] R. Kubo, J. Phys. Soc. Jpn. 17 (1962) 1100–1120.

[22] S.P. Neshyba, R. Lynch, R.R. Gamache, T. Gabard, J.-P. Champion, J. Chem. Phys. 101 (1994) 9412–9421.

[23] R.R. Gamache, L. Rosenmann, J. Mol. Spectrosc. 164 (1994) 489–499.

[24] S.L. Shostak, J.S. Muenter, J. Chem. Phys. 94 (1991) 5883–5890.

[25] Y. Luo, H. Agren, O. Vahtras, P. Jorgensen, V. Spirko, H. Hettema, J. Chem. Phys. 98 (1993) 7159–7164.

[26] J.E. Jones, Proc. R. Soc. A 106 (1924) 463–477.

[27] J.O. Hirschfelder, C.F. Curtiss, R.B. Bird, Molecular Theory of Gases and Liquids, Wiley, New York, 1964.

[28] R.J. Good, C.J. Hope, J. Chem. Phys. 55 (1971) 111–116.

[29] R.A. Sack, J. Math. Phys. 5 (1964) 260–268.

[30] S.P. Neshyba, R.R. Gamache, J. Quant. Spectrosc. Radiat. Transfer 50 (1993) 443–453.

[31] J.K.G. Watson, J. Chem. Phys. 46 (1967) 1935–1949.

[32] F. Matsushima, H. Odashima, T. Iwaskai, S. Tsunekawa, J. Mol. Struct. 352–353 (1995) 371–378.

[33] J.-M. Flaud, C. Camy-Peyret. Watson Hamiltonian constants for low lying vibrational states of H_2O, 2005.

[34] C. Camy-Peyret, J.-M. Flaud, J. Mol. Spectrosc. 59 (1976) 327–337.

[35] W.H. Flygare, R.C. Benson, Mol. Phys. 20 (1971) 225–250.

[36] D.R. Lide, (Ed.), CRC Handbook of Physics and Chemistry, 83rd ed., The Chemical Rubber Company, Clevland, OH, 2003.

[37] L.S. Rothman, A. Barbe, D.C. Benner, L.R. Brown, C. Camy-Peyret, M.R. Carleer, K. Chance, C. Clerbaux, V. Dana, V.M. Devi, A. Fayt, J.-M. Flaud, R.R. Gamache, A. Goldman, D. Jacquemart, K.W. Jucks, W.J. Lafferty, J.-Y. Mandin, S.T. Massie, V. Nemtchinov, D.A. Newnham, A. Perrin, C.P. Rinsland, J. Schroeder, K.M. Smith, M.A.H. Smith, K. Tang, R.A. Toth, J.V. Auwera, P. Varanasi, K. Yoshino, J. Quant. Spectrosc. Radiat. Transfer 82 (2003) 5–44.

[38] J.Y. Mandin, J.-M. Flaud, C. Camy-Peyret, J. Quant. Spectrosc. Radiat. Transfer 23 (1980) 351–370.

[39] J.Y. Mandin, J.-M. Flaud, C. Camy-Peyret, J. Quant. Spectrosc. Radiat. Transfer 26 (1981) 483–494.

[40] V.M. Devi, D.C. Benner, C.P. Rinsland, M.A.H. Smith, B.D. Sidney, J. Mol. Spectrosc. 117 (1986) 403–407.

[41] F.M. Nicolaisen, Workshop paper 5.8, in: Y. Ponomerev (Ed.), Atmospheric Spectroscopy Applications Workshop, Moscow, USSR, 1990.

[42] V.M. Devi, B. Fridovich, G.D. Jones, D.G.S. Snyder, J. Mol. Spectrosc. 111 (1985) 114–118.

[43] R.S. Eng, P.L. Kelley, A. Mooradian, A.R. Calawa, T.C. Harman, Chem. Phys. Lett. 19 (1973) 524–528.

[44] R.S. Eng, A.W. Mantz, J. Mol. Spectrosc. 74 (1979) 388–399.

[45] Y. Ben Aryeh, J. Quant. Spectrosc. Radiat. Transfer 7 (1967) 211–224.

[46] J.R. Izatt, H. Sakai, W.S. Benedict, J. Opt. Soc. Am. 59 (1969) 19–26.

[47] M.A. Guerra, M. Ketabi, A. Sanchez, M.S. Feld, A. Javan, J. Chem. Phys. 63 (1975) 1317–1319.

[48] J.A. Mucha, Appl. Spectrosc. 36 (1982) 141–147.

[49] R.S. Eng, P.L. Kelley, A.R. Calawa, T.C. Harman, K.W. Nill, Mol. Phys. 28 (1974) 653–664.

[50] J.M. Hartmann, J. Taine, J. Bonamy, B. Labani, D. Robert, J. Chem. Phys. 86 (1987) 144–156.

[51] J.J. Remedios, PhD thesis, Physics, University of Oxford, 1990.

[52] R.A. Toth, L.R. Brown, C. Plymate, J. Quant. Spectrosc. Radiat. Transfer 59 (1998) 529–562.

[53] R.R. Gamache, J.-M. Hartmann, J. Quant. Spectrosc. Radiat. Transfer 83 (2004) 119–147.

[54] R.R. Gamache, J. Mol. Spectrosc. 229 (2005) 9–18.

[55] G. Wagner, M. Birk, R.R. Gamache, J.-M. Hartmann, J. Quant. Spectrosc. Radiat. Transfer 92 (2005) 211–230.

[56] R.A. Toth, L.R. Brown, M.A.H. Smith, V. Malathy Devi, D. Chris Benner, M. Dulick, J. Quant. Spectrosc. Radiat. Transfer 101 (2006) 339–366.

[57] G. Birnbaum, Adv. Chem. Phys. 12 (1967) 487–548.